

## Highly Selective Detection of TNP over other Nitro Compounds in Water: Role of Selective Host-Guest Interactions in Zr-NDI MOF

Govu Radha,<sup>a</sup> T. Leelasree,<sup>a</sup> D. Muthukumar,<sup>b</sup> Renjith S. Pillai<sup>b</sup> and Himanshu Aggarwal\*<sup>a</sup>

<sup>a</sup>Department of Chemistry, Birla Institute of Technology and Science, Hyderabad Campus, Hyderabad 500078, India. Email: himanshu.aggarwal@hyderabad.bits-pilani.ac.in

<sup>b</sup>Department of Chemistry, SRM Institute of Science and Technology, SRM Nagar, Kattankulathur-603 203, Chennai, Tamil Nadu, India.

### Scheme of ligand (BINDI) synthesis

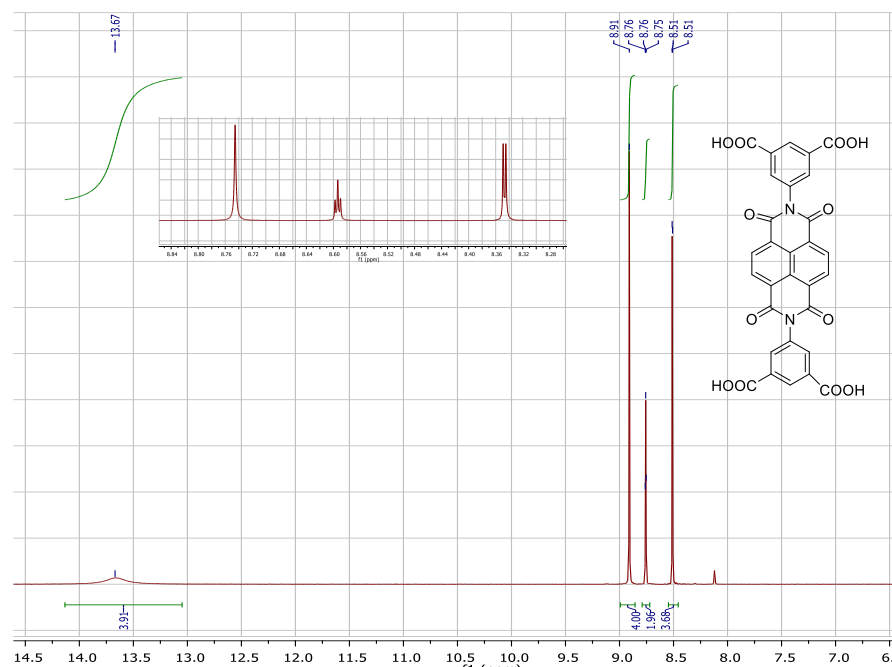
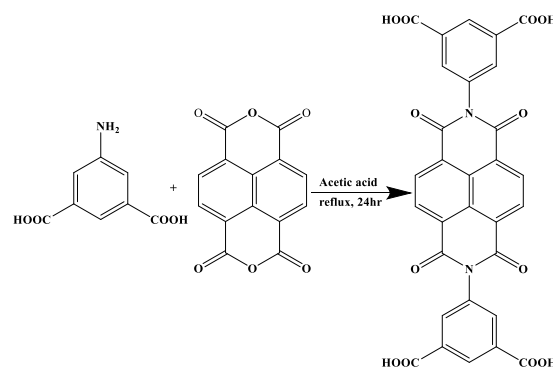


Figure S1: The  $^1\text{H}$  NMR spectra of Bindi in  $\text{DMSO-d}_6$ .

**Table S1.** Crystallographic data of **1**.

Identification code	HA_MOF1
Empirical formula	C <sub>17</sub> H <sub>15</sub> NO <sub>18</sub> Zr <sub>3</sub>
Formula weight	794.975
Temperature/K	100.0
Crystal system	orthorhombic
Space group	Ibam
a/Å	21.4898(12)
b/Å	25.2933(9)
c/Å	33.1199(16)
α/°	90
β/°	90
γ/°	90
Volume/Å <sup>3</sup>	18002.3(15)
Z	16
ρ <sub>calc</sub> g/cm <sup>3</sup>	1.173
μ/mm <sup>-1</sup>	6.051
F(000)	6221.3
Crystal size/mm <sup>3</sup>	0.05 × 0.025 × 0.025
Radiation	Cu Kα ( $\lambda = 1.54184$ )
2Θ range for data collection/°	8.22 to 143.5
Index ranges	-25 ≤ h ≤ 26, -30 ≤ k ≤ 30, -39 ≤ l ≤ 20
Reflections collected	54320
Independent reflections	8831 [R <sub>int</sub> = 0.1153, R <sub>sigma</sub> = 0.0568]
Data/restraints/parameters	8831/0/365
Goodness-of-fit on F <sup>2</sup>	1.100
Final R indexes [I>=2σ (I)]	R <sub>1</sub> = 0.0702, wR <sub>2</sub> = 0.1954
Final R indexes [all data]	R <sub>1</sub> = 0.0964, wR <sub>2</sub> = 0.2362
Largest diff. peak/hole / e Å <sup>-3</sup>	2.12/-1.85
CCDC number	2067442

### **Computational Details:**

First, the experimentally elucidated **1** containing  $\mu_3$ -bridged oxygen atoms, and Zr metal site having hydroxyl group and water molecule in the framework consisting of a carboxylate ligand were modelled (Figure 24a). The resulting MOF was structural optimized by the Density Functional theory (DFT) using the Perdew-Burke-Ernzerhof (PBE) functionals<sup>1,2</sup> in Quickstep module of CP2K package.<sup>3-6</sup> For the structural optimization, the cell parameters of the framework as obtained from the experiment were kept constant, however the framework atoms have been relaxed for the geometry optimization. Here, for hydrogen, oxygen, nitrogen and carbon atoms, triple-zeta potential (TZVP-MOLOPT)<sup>7</sup> basis set has been considered while the Zirconium atom has double-zeta potential basis set (DZVP-MOLOPT).<sup>7</sup> The pseudo potentials used for all of the atoms were those derived by Goedecker, Teter and Hutter.<sup>8</sup> The van der Waals effects interactions were taken into account via the use of semi-empirical dispersion corrections as implemented in the DFT-D3 method. In the same way, the substrate 2,4,6-trinitro phenol (Figure S24b) and 2,4-dinitro toluene (Figure S24c) has been optimized with the same DFT level and parameters using Quickstep module of CP2K package.<sup>3-6</sup> Later, the substrate 2,4,6-TNP has been loaded consecutively (Figure S25) in pore channels of the MOF for obtaining the substrate loaded **1**. The final loaded MOF models were then geometry-optimized using the Quickstep module of the CP2K package and considering the same level of theory and parameters as for the optimization of the **1**. All the atomic coordinates of the MOF models were relaxed and all the calculations were performed at the  $\Gamma$ -point. Finally, the geometry optimized **1** without and with analytes were used to explore the single point energy and further extraction of HOMO and LUMO energy for understanding the optical properties of the TNP and DNT loaded **1** with the same level of theory and parameters as for the optimization of the **1**. Table S6 and S7 represents the HOMO and LUMO energy level for analyte loaded **1** and different number of 2,4,6-TNP molecules. Figures S25 and S26 represents the HOMO and LUMO

energy plot for analyte loaded MOF and 2,4,6-TNP molecules, respectively whereas Figure S27 represents the HOMO-LUMO energy plot for **1**, DNT substrate and DNT loaded **1** Figure S28 and the energy values for DNT substrate and Zr-MOF loaded with single DNT substrate has been represented in the Table S8.

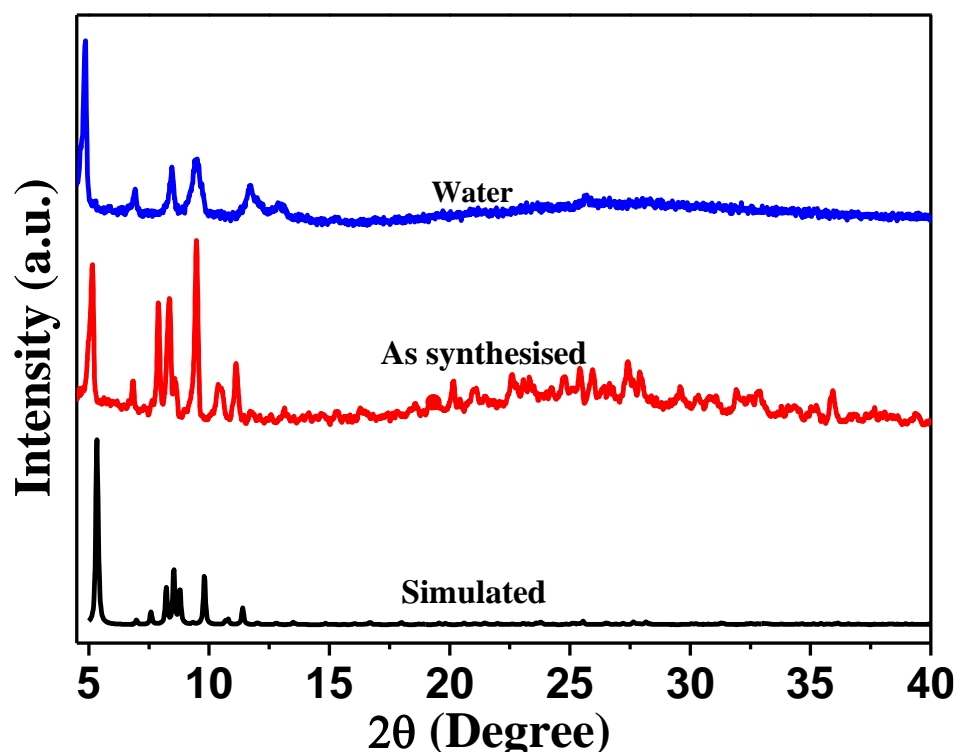


**Figure S2:** PXRD pattern showing the stability of **1** when exposed to water for 24 hr.

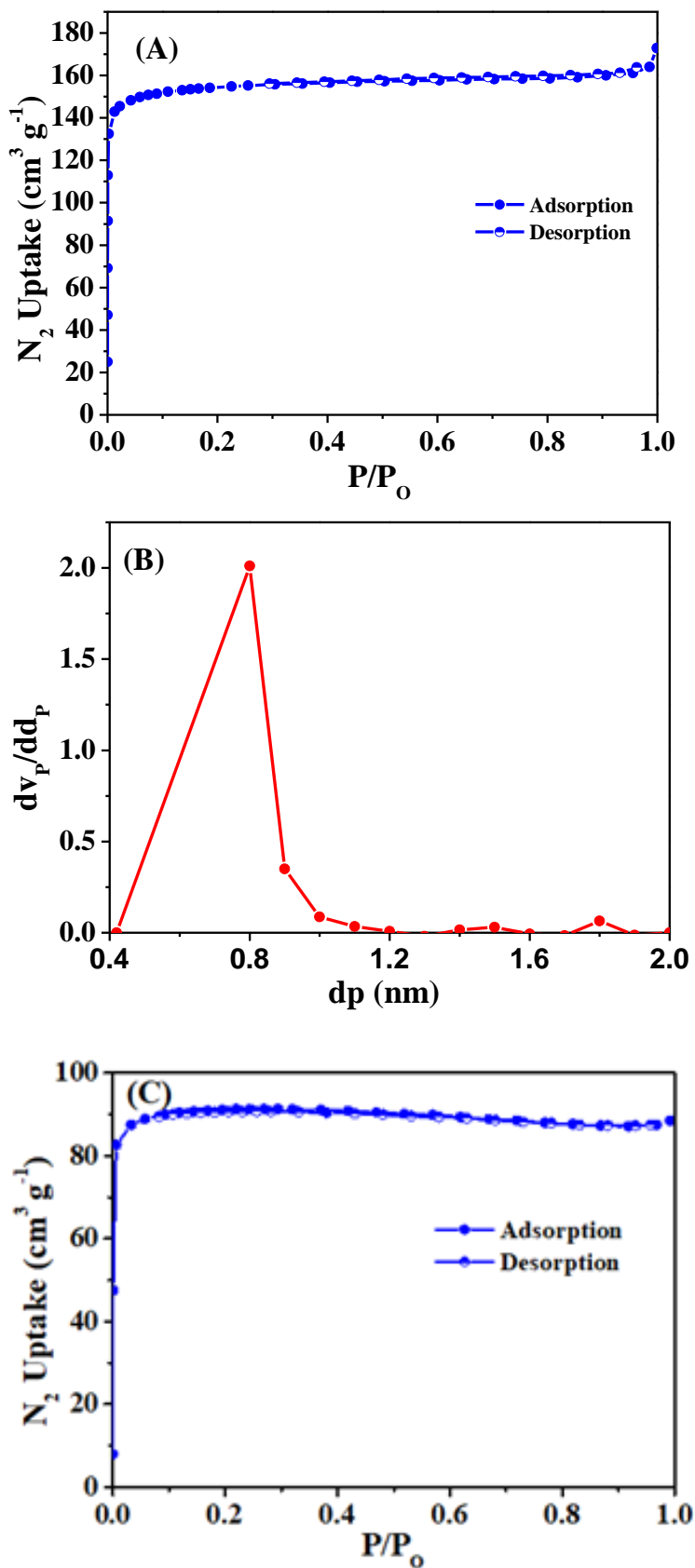


**Figure S3:** (A) Adsorption isotherm of **1** and (B) pore diameter of **1** and (c) Adsorption isotherm of **1** after sensing experiment with TNP at 77K.

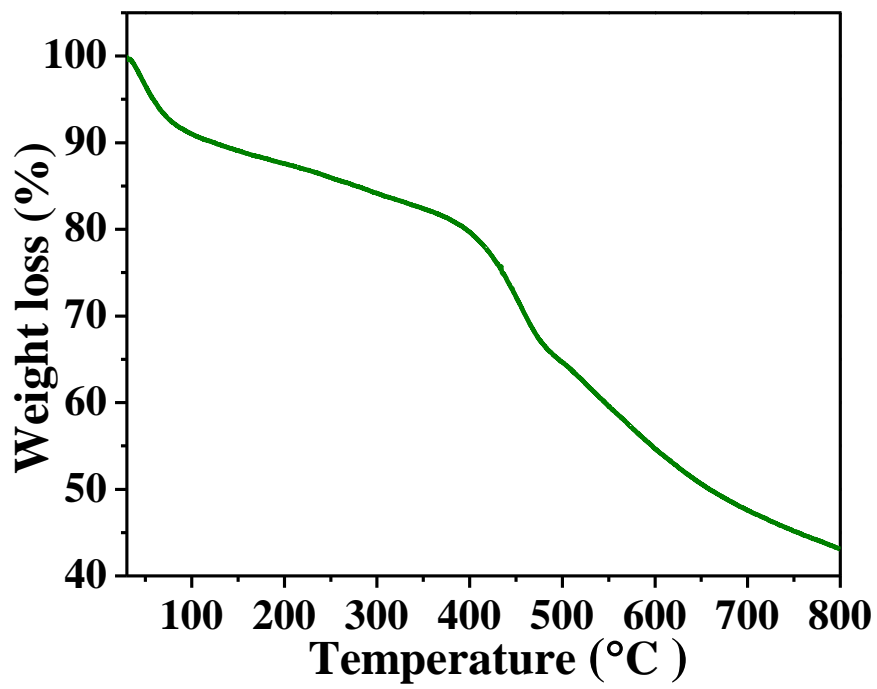


**Figure S4:** Thermogravimetric analysis of **1**.

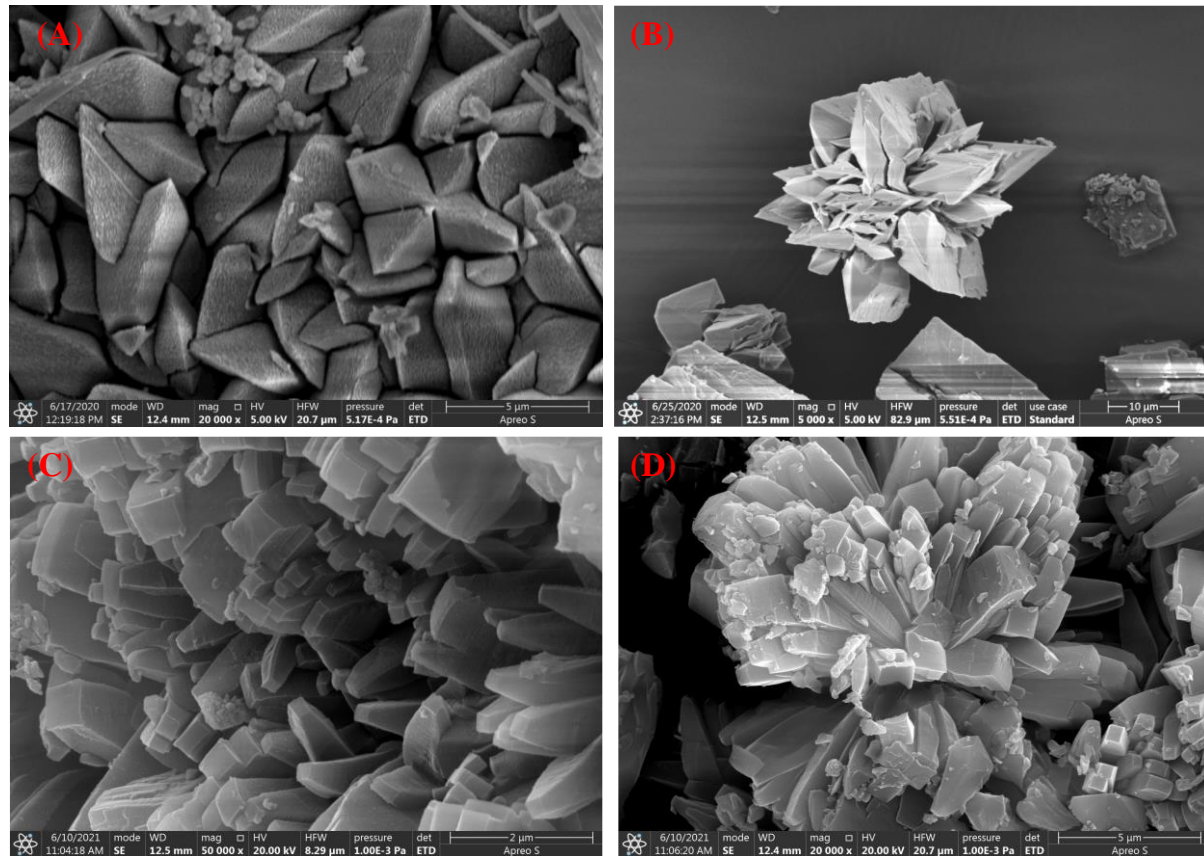


**Figure S5:** SEM image showing inter-grown rods of **1** (A, B) As synthesised material and (C, D) After sensing experiments with TNP.

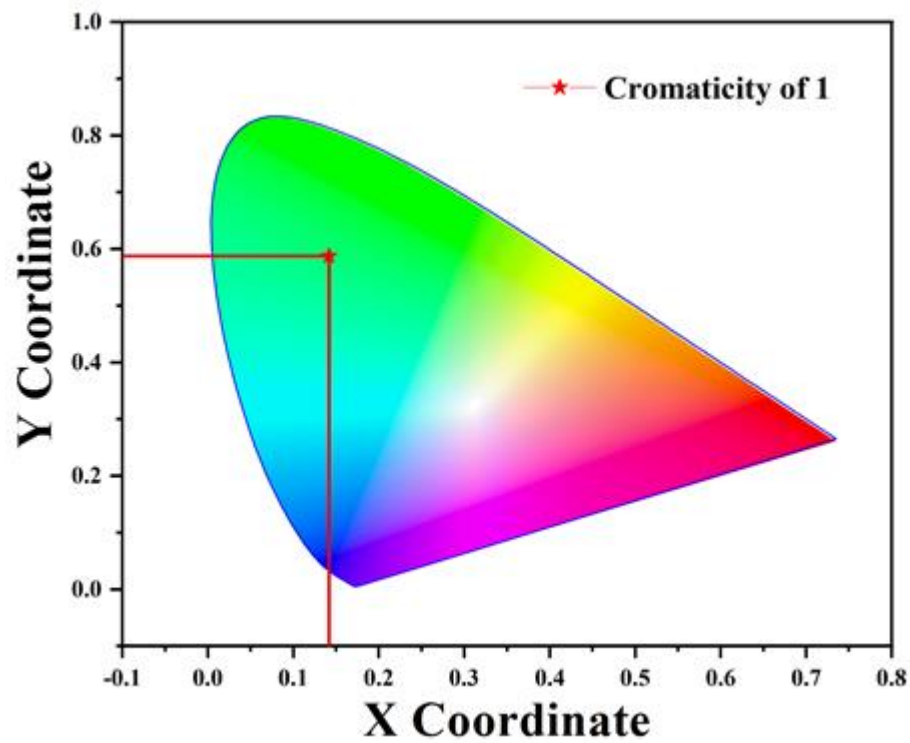


**Figure S6.** Commission Internationale de l'eclairage (CIE) chromaticity diagram of MOF 1.

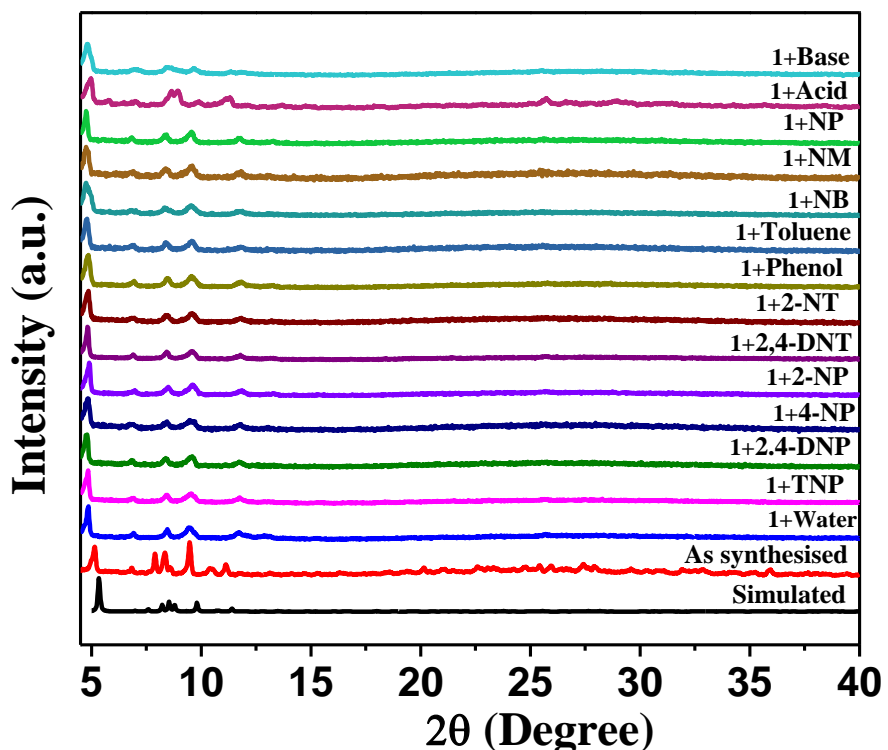


**Figure S7.** PXRD patterns showing stability of **1** in the presence of different nitro compounds, acid and base.

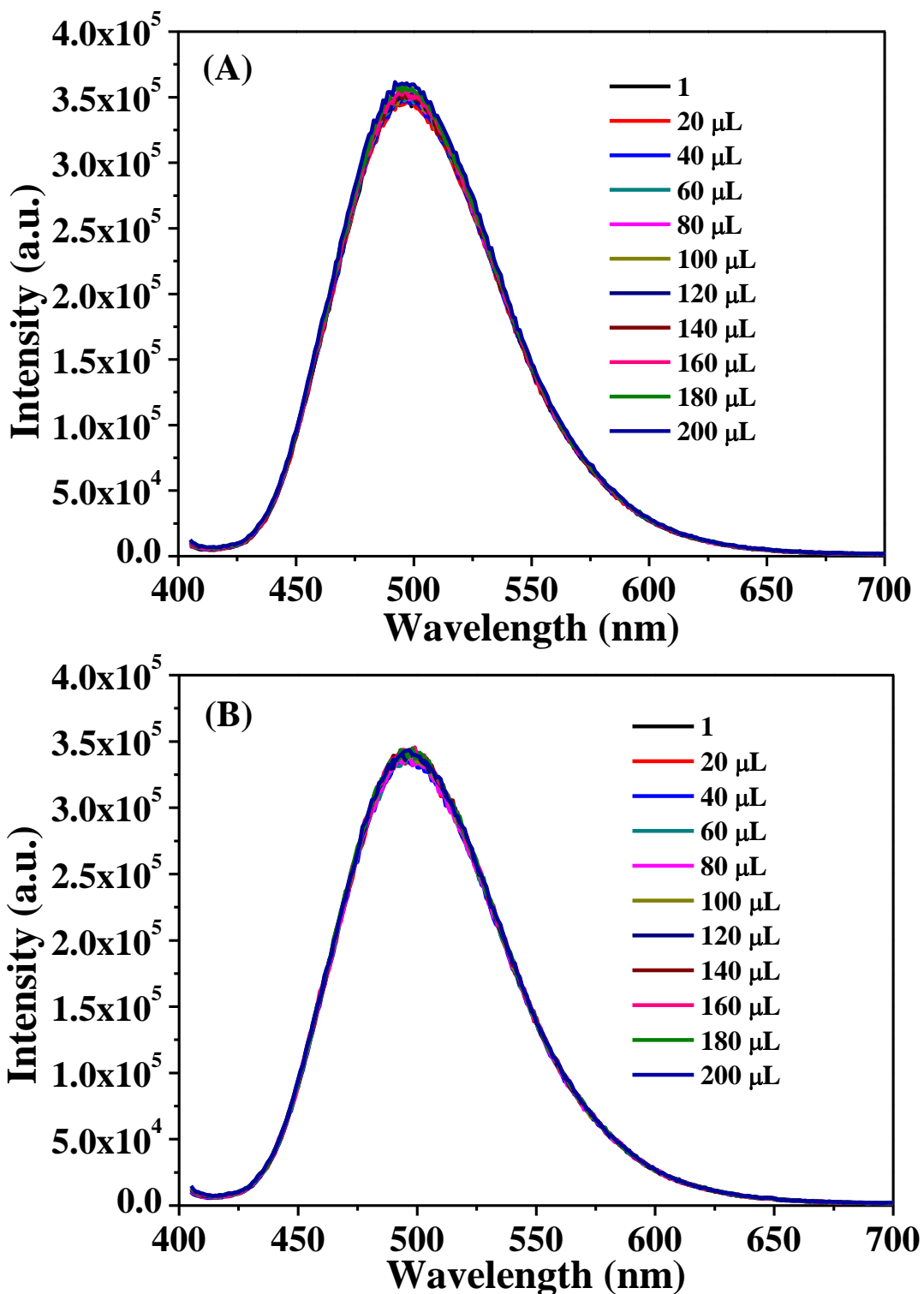


**Figure S8:** Emission spectra of **1** dispersed in water upon incremental addition of (A) NM (5 mM) and (B) NP in water ( $\lambda_{\text{ex}}=395$  nm).

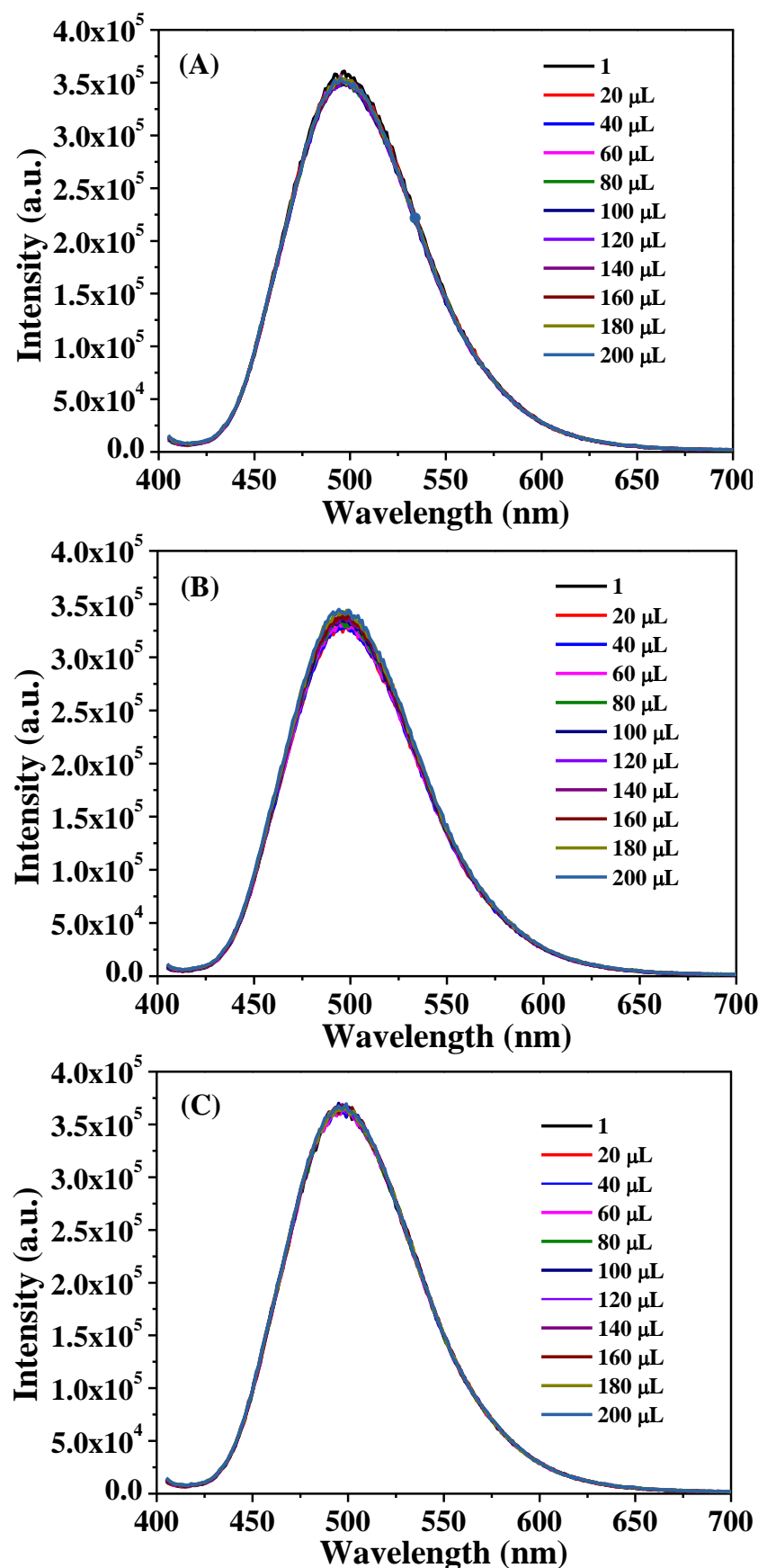


**Figure S9:** Emission spectra of **1** dispersed in water upon incremental addition of (A) Phenol (5 mM), (B) Toluene (5 mM) and (c) NB (5 mM) in water ( $\lambda_{\text{ex}}=395$  nm).

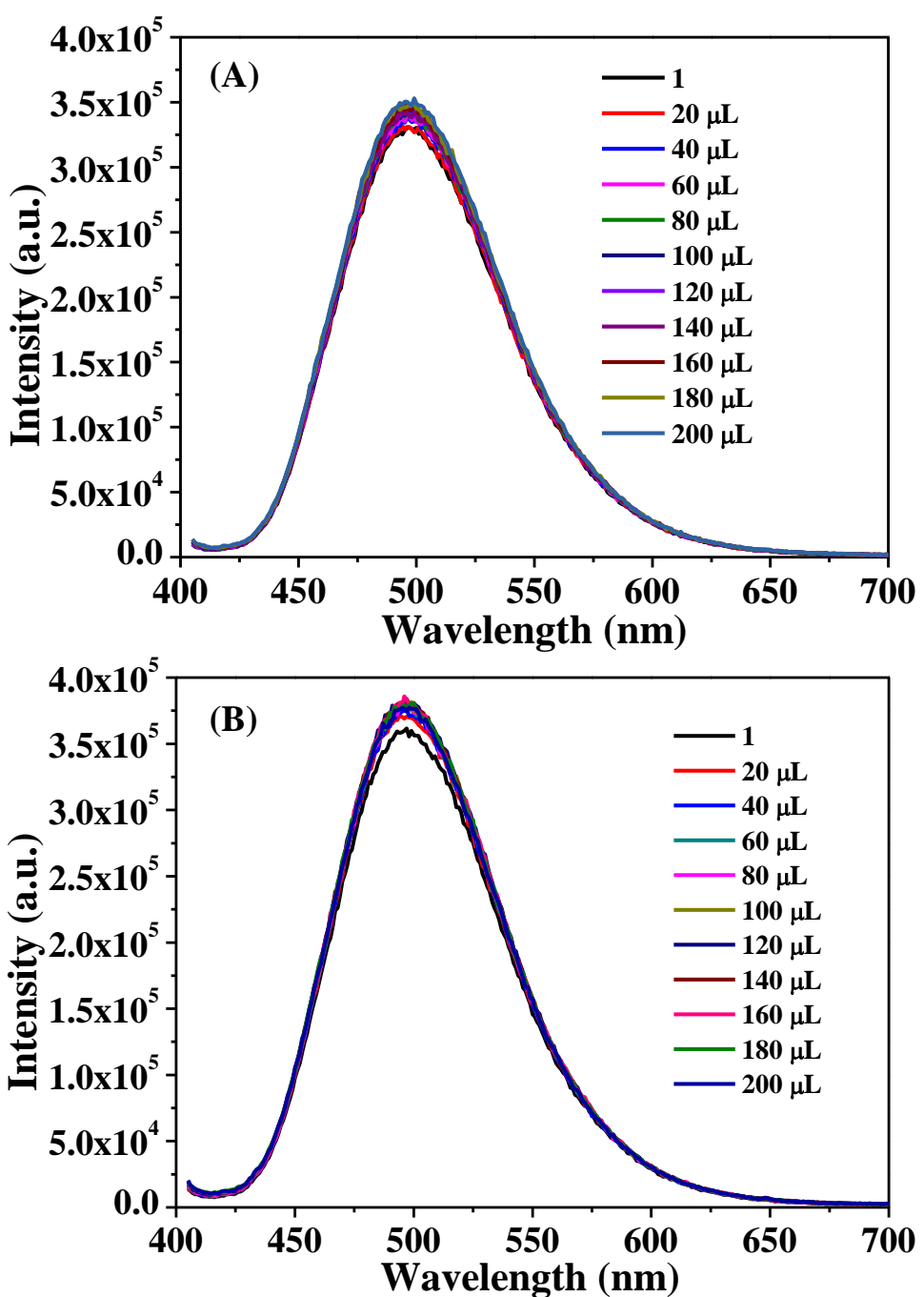


**Figure S10:** Emission spectra of **1** dispersed in water upon incremental addition of (A) 2,4-DNT (5 mM) and (B) 2-NT (5 mM) in water ( $\lambda_{\text{ex}}=395$  nm).

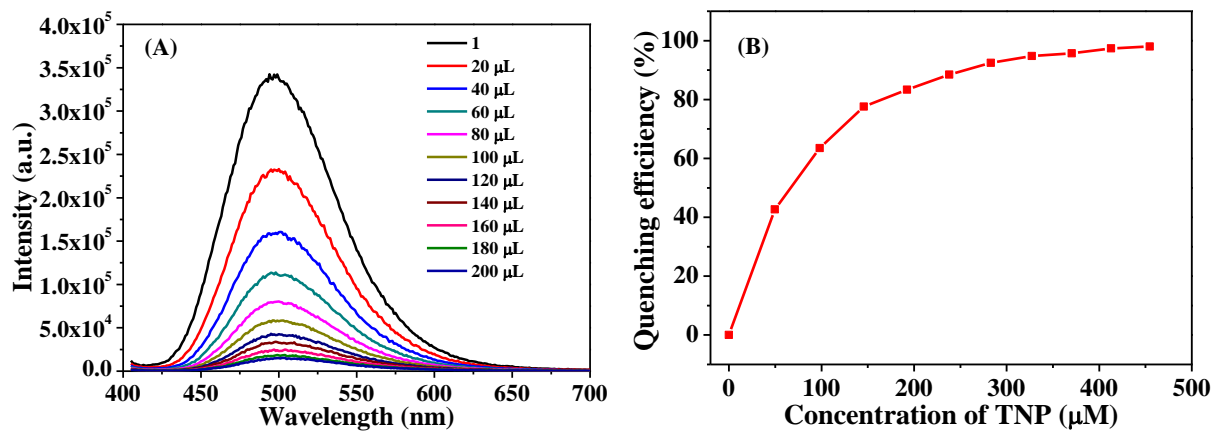


**Figure S11:** (A) Emission spectra of **1** dispersed in water upon incremental addition of TNP (5 mM) in water ( $\lambda_{\text{ex}}=395$  nm). (B) Quenching efficiency of TNP.

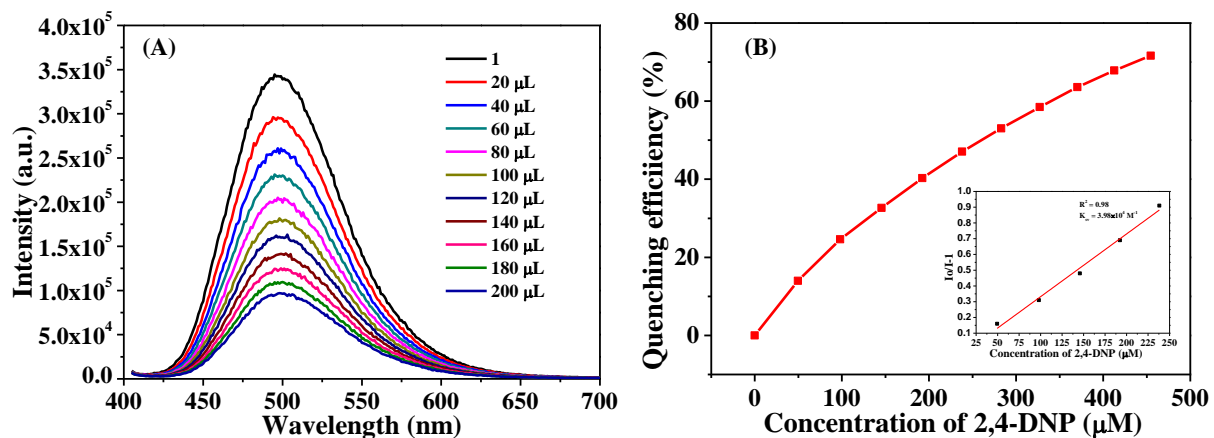


**Figure S12:** (A) Emission spectra of **1** dispersed in water upon incremental addition of 2,4-DNP (5 mM) in water ( $\lambda_{\text{ex}}=395$  nm). (B) Quenching efficiency of 2,4-DNP (Inset Stern Volmer plot).

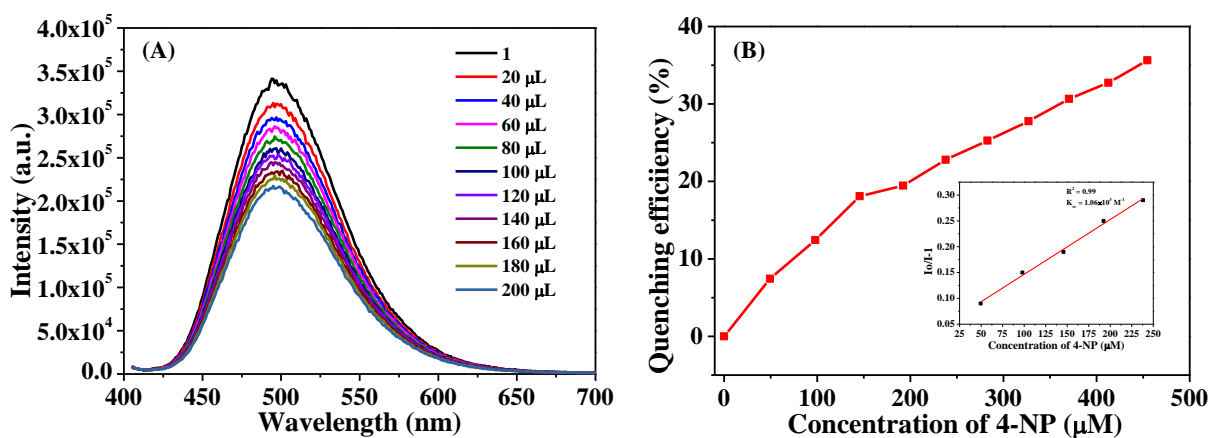


**Figure S13:** (A) Emission spectra of **1** dispersed in water upon incremental addition of 4-NP (5 mM) in water ( $\lambda_{\text{ex}}=395$  nm). (B) Quenching efficiency of 4-NP (Inset Stern Volmer plot).

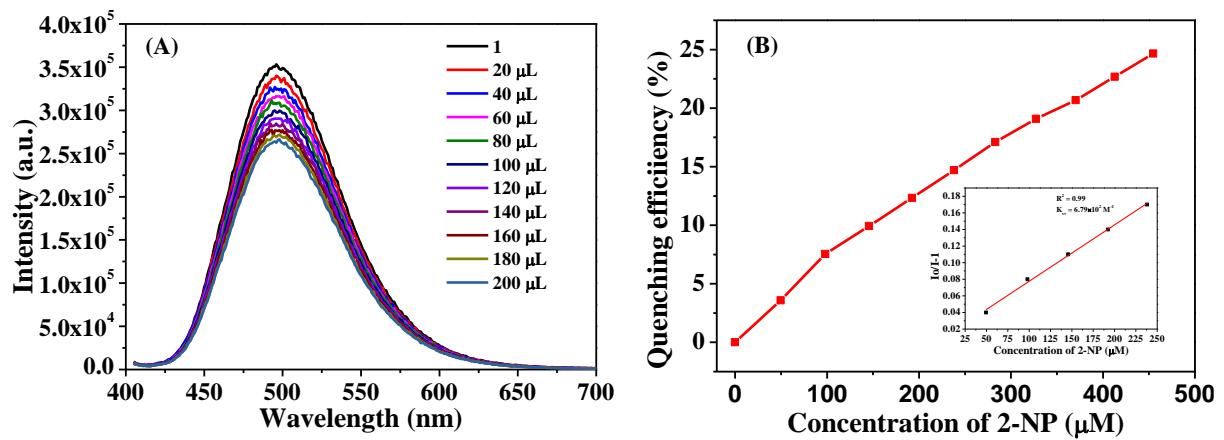


**Figure S14:** (A) Emission spectra of **1** dispersed in water upon incremental addition of 2-NP (5 mM) in water ( $\lambda_{\text{ex}}=395$  nm). (B) Quenching efficiency of 2-NP (Inset Stern Volmer plot).

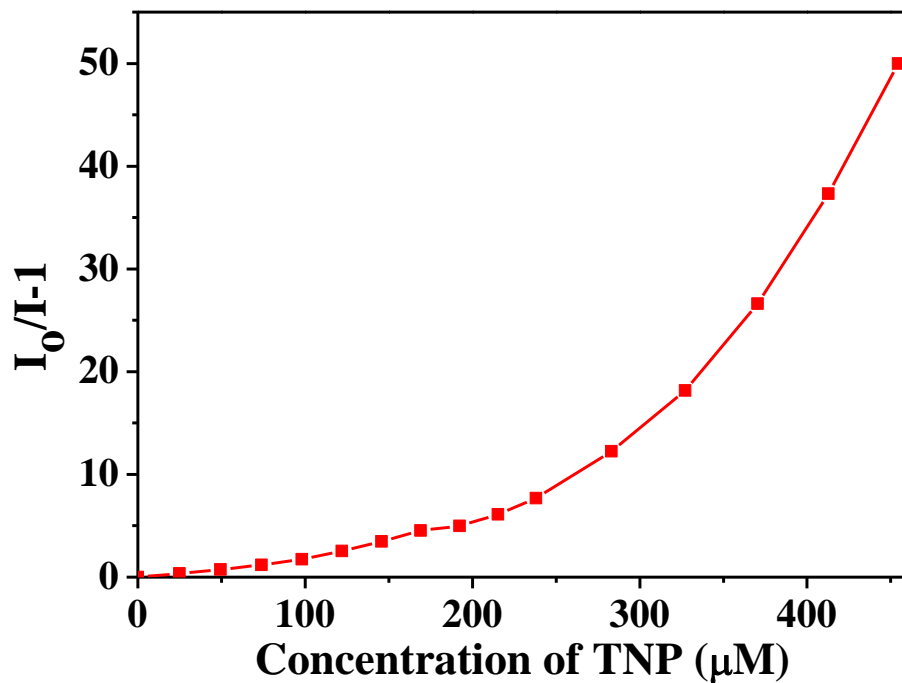


**Figure S15:** Stern Volmer plot of **1** upon incremental addition of TNP (5mm) in water.

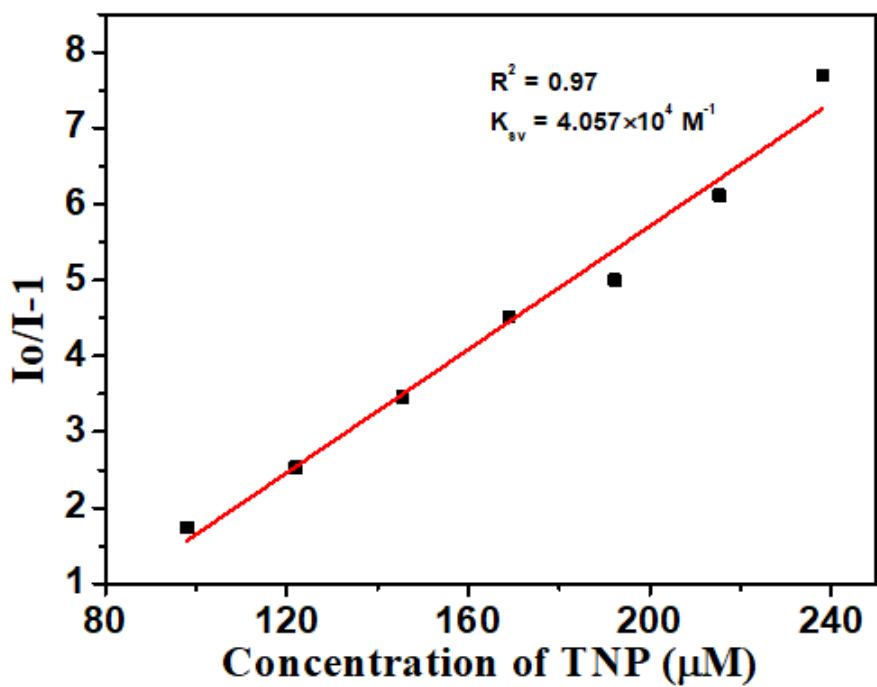


**Figure S16:** Linear range Stern Volmer plot of **1** upon incremental addition of TNP (5mm) in aqueous solution.

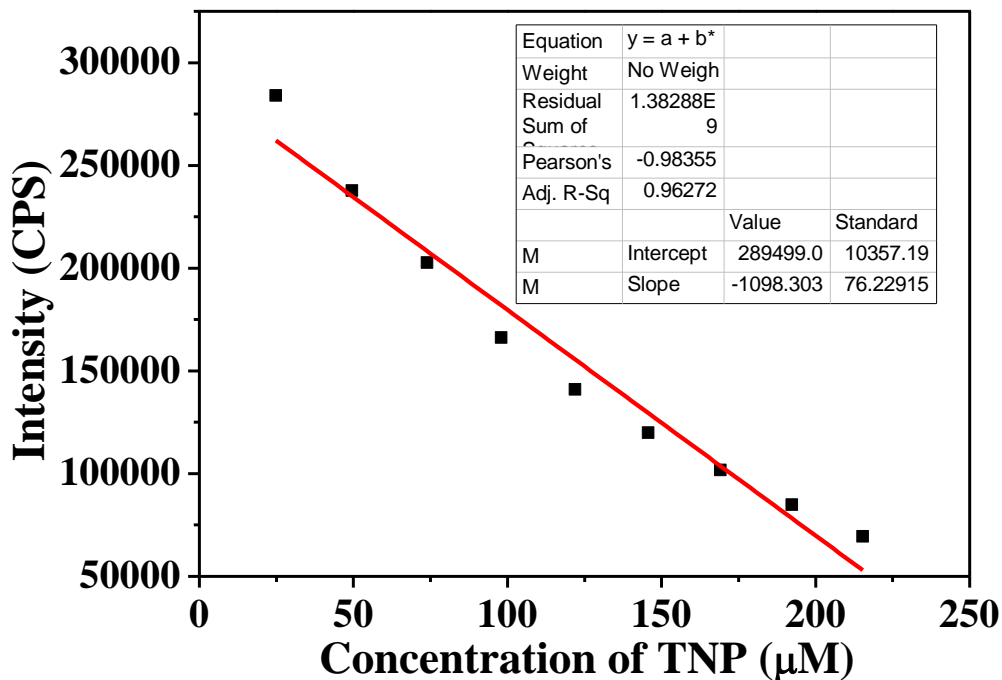


**Figure S17:** Linear regression curve of fluorescence intensity of **1** upon incremental addition of TNP (5 mM) in aqueous solution.

**Table S2:** Blank fluorescence intensity values of **1** and limit of detection of TNP.

S NO	Fluorescence intensity (cps)
<b>Reading 1</b>	368500.851
<b>Reading 2</b>	389767.442
<b>Reading 3</b>	399000
<b>Reading 4</b>	396282.048
<b>Reading 5</b>	399152.542
<b>Standard deviation (<math>\sigma</math>)</b>	<b>12894.18016</b>
<b>Slope (m)</b>	<b>1098.303 <math>\mu\text{M}^{-1}</math></b>
<b>Detection limit (<math>3\sigma/m</math>)</b>	<b>35.22 <math>\mu\text{M}</math></b>
<b>Limit of detection</b>	<b>8.069 ppm</b>

**Table S3:** Comparison of selective detection of TNP, LOD and QE reported for various MOF materials.

S NO	MOF	$K_{sv} (\text{M}^{-1})$	LOD	QE	Absolute selective detection of TNP	Reference
<b>1</b>	$\text{Zr}_6\text{O}_4(\text{OH})_4(\text{L})_6$ (UiO-67@N)	$2.9 \times 10^4$		73%	No	[10]
<b>2</b>	$[\text{Cd}(5\text{-BrIP})(\text{TIB})]\text{n}$	$2.68 \times 10^4$	$0.27 \mu\text{M}$	84.5%	No	[11]
<b>3</b>	BUT-12	$2.1 \times 10^4$	23 ppb		No	[12]
	BUT-13	$1 \times 10^4$	12 ppb			
<b>4</b>	$[\text{Zn}_4(\text{DMF})(\text{Ur})_2(\text{NDC})_4]$	$10.83 \times 10^4$	1.63 ppm		No	[13]
<b>5</b>	$[\text{Zr}_6\text{O}_4(\text{OH})_4(\text{BTDB})_6] \cdot 8\text{H}_2\text{O} \cdot 6\text{DMF}$	$2.49 \times 10^4$	$1.63 \times 10^{-6} \text{ M}$	98%	No	[14]
<b>6</b>	$[\text{Cd}(\text{NDC})0.5(\text{PCA})]\text{Gx}$	$3.5 \times 10^4$		78%	No	[15]
<b>7</b>	UiO-68@NH <sub>2</sub>	$5.8 \times 10^4$	0.4 ppm	86%	No	[16]
<b>8</b>	$\text{Cd}_2(\text{PAM})_2(\text{dpe})_2(\text{H}_2\text{O})_2 \cdot 0.5(\text{dpe})$		$1.76 \times 10^{-6} \text{ gL}^{-1}$	98.4%	No	[17]
<b>9</b>	$\{\text{Tb}(\text{L})_{1.5}(\text{H}_2\text{O})\} \cdot 3\text{H}_2\text{O}\text{n}$		$7.47 \times 10^4 \text{ M}^{-1}$		No	[18]
<b>10</b>	<b>Zr-NDI MOF (1)</b>	<b><math>4.057 \times 10^4</math></b>	<b><math>8.069 \text{ ppm}</math> <b>(8.1 ppm)</b></b>	<b>95%</b>	<b>Yes</b>	<b>This work</b>

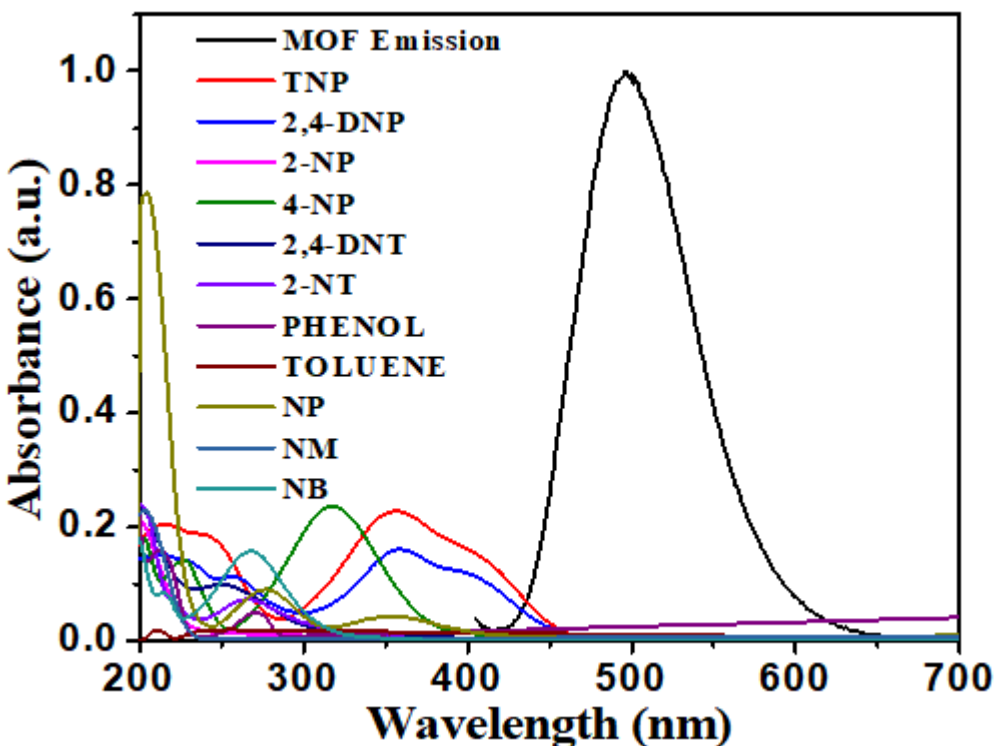


**Figure S18:** Spectral overlap between emission ( $\lambda_{\text{ex}}=395$  nm) of **1** and absorption spectra of analytes.

**Table S4:** Lifetime decay profile values of **1** upon incremental addition of TNP (5 mM aqueous solution).

sample	$\tau_1$ (ns)	$\tau_2$ (ns)	$\tau_3$ (ns)	$\alpha_1$	$\alpha_2$	$\alpha_3$	$\chi^2$	Average lifetime (ns)
MOF	1.81	4.64	0.20	0.18	0.09	0.17	1.12	2.83
MOF+40 $\mu\text{L}$ TNP	1.44	3.64	0.19	0.17	0.08	0.75	1.09	2.13
MOF+80 $\mu\text{L}$ TNP	1.29	3.15	0.20	0.16	0.06	0.78	1.01	1.60
MOF+120 $\mu\text{L}$ TNP	1.03	2.57	0.17	0.12	0.04	0.83	1.07	1.16
MOF+160 $\mu\text{L}$ TNP	0.80	2.10	0.15	0.10	0.04	0.86	1.23	0.87
MOF+200 $\mu\text{L}$ TNP	0.49	1.67	0.07	0.09	0.03	0.88	1.26	0.65

### Temperature Dependent Fluorescence Experiments:

The fluorescence experiments were performed at different temperatures where TNP was added in incremental manner to **1**. (Fig. S19) It was observed that with an increase in the temperature, there was an increase in the  $K_D$  value where D refers to dynamic. (Fig. S19-S20, Table S5) This confirms the operation of dynamic quenching mechanism in this case.<sup>19</sup>

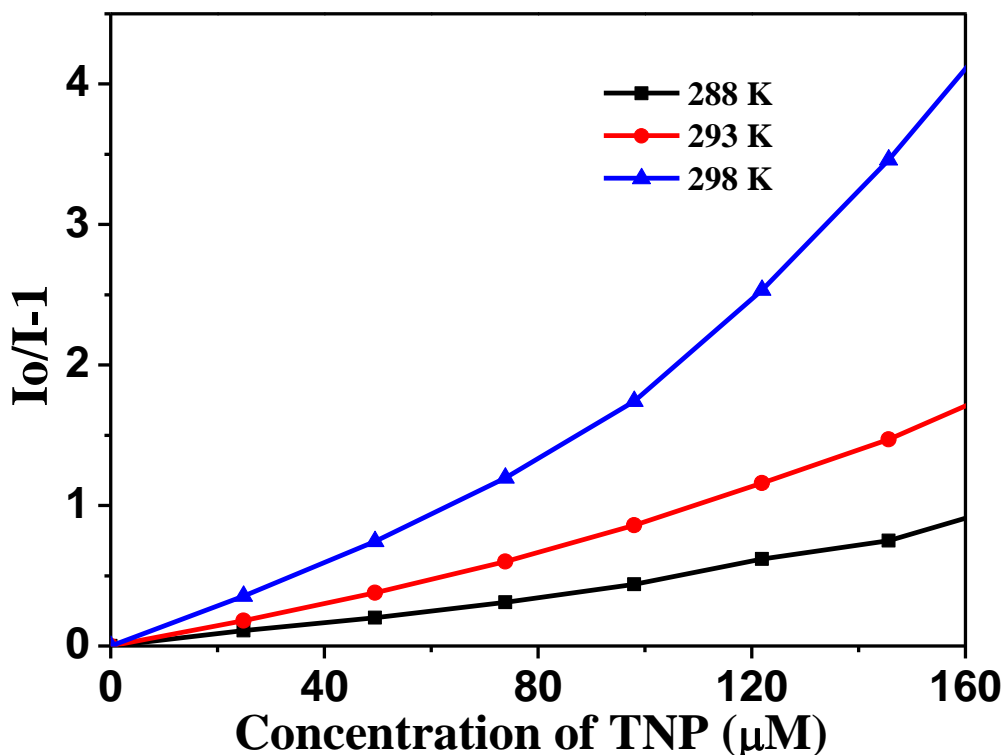


**Figure S19:** Stern Volmer plot of **1** upon incremental addition of TNP (5 mM) at different temperatures.

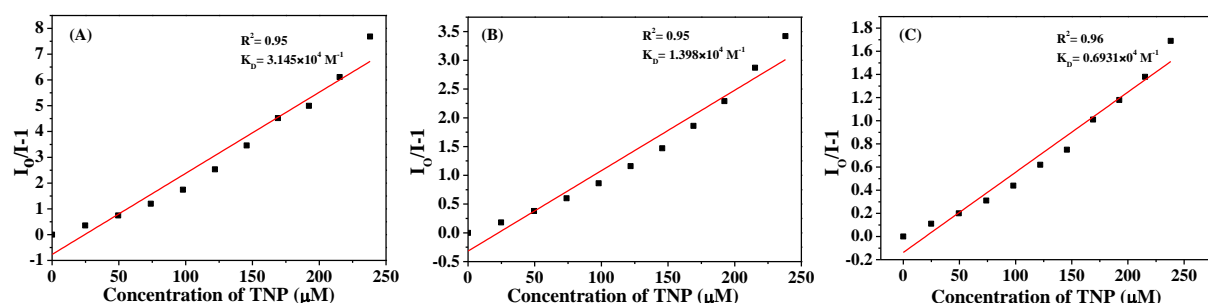


**Figure S20:** Stern Volmer plot of **1** upon incremental addition of TNP (5 mM) at different temperatures (A) 288 K, (B) 293 K and (C) 298 K.

**Table S5:**  $K_D$  values of **1** upon addition of TNP (5 mM) aqueous solution at different temperatures.<sup>19</sup>

Temperature (°C)	$K_D$ ( $M^{-1}$ )
15	$0.6931 \times 10^4$
20	$1.398 \times 10^4$
25	$3.145 \times 10^4$

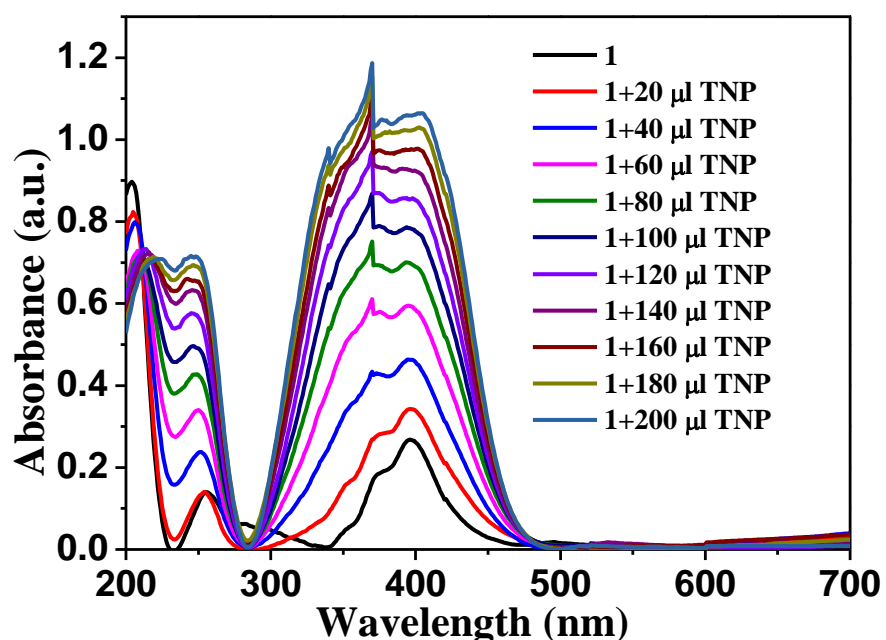


**Figure S21:** Absorption spectra of **1** dispersed in water upon incremental addition of TNP (5 mM) in water.

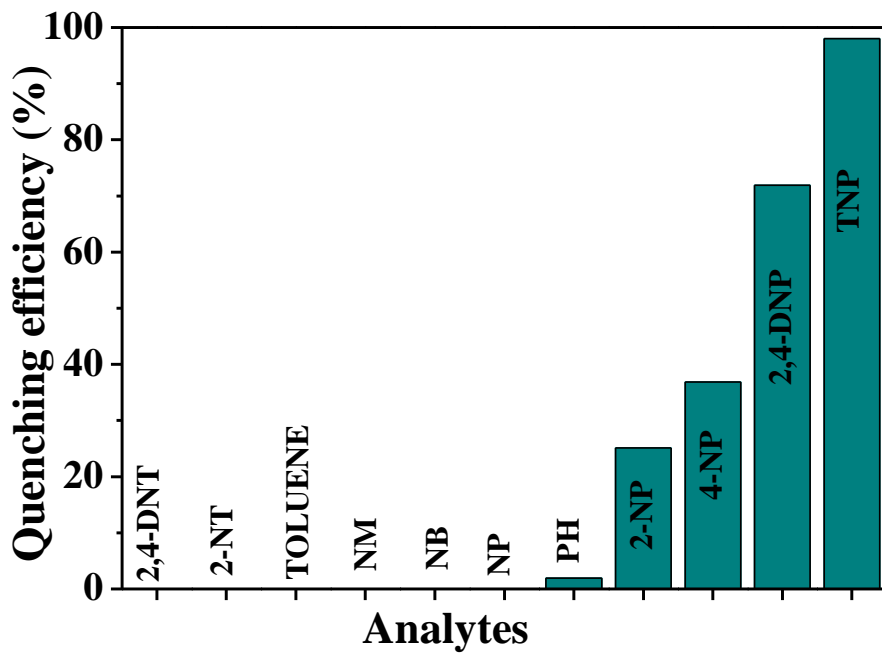


**Figure S22:** Quenching efficiency of analytes upon addition of 200  $\mu\text{L}$  of each analyte to the **1** in aqueous suspension.

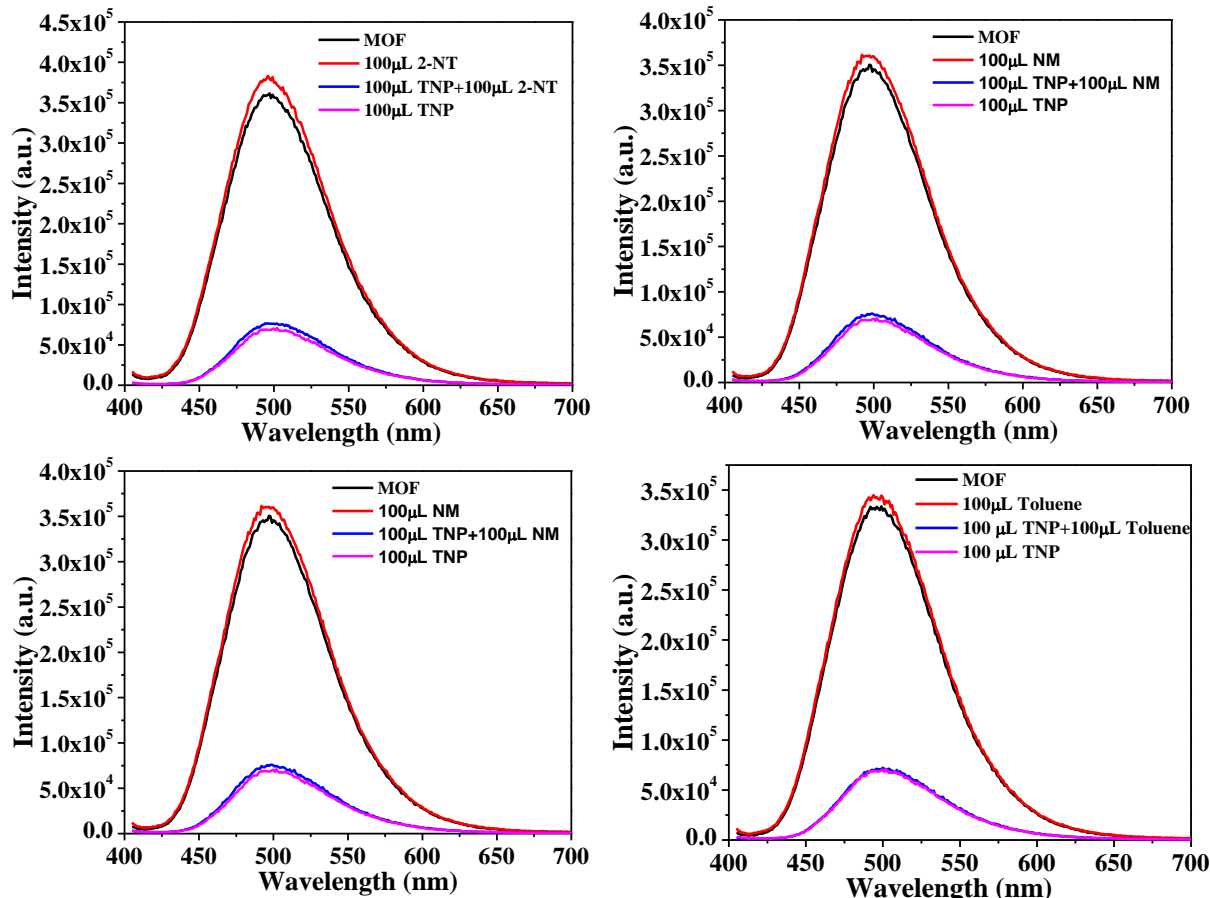


**Figure S23:** Selectivity studies of analytes against TNP upon addition of (1:1 v/v) TNP + analytes (5 mM) to **1** in aqueous suspension ( $\lambda_{\text{ex}}=395 \text{ nm}$ ).

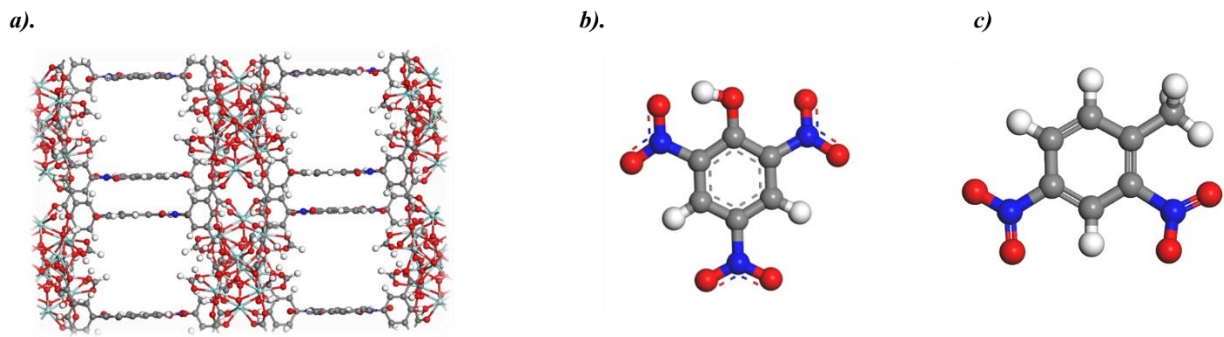


**Figure S24.** The single unit cell ( $1 \times 1 \times 1$  simulation box) viewed along *a* direction for **1** (a), 2,4,6-trinitro-phenol (b) and 2,4-dinitro toluene (c) considered for the DFT calculations. (Grey-Carbon; Blue-Nitrogen; White-Hydrogen; Red-Oxygen; Cyan-Zr)

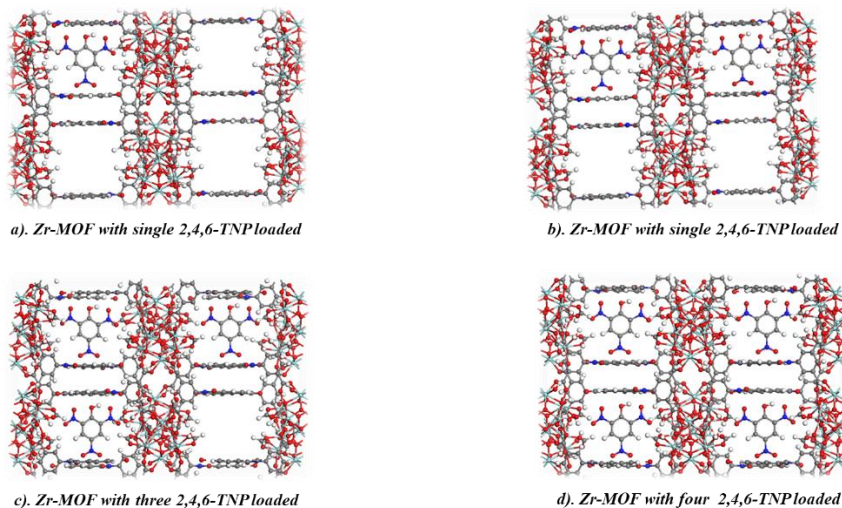


**Figure S25.** DFT-optimized Zr-MOF with TNP analytes with **1** (a), 2 (b), 3 (c) and 4 (d) molecule per unit cell viewed along *a* direction. (Grey-Carbon; Blue-Nitrogen; White-Hydrogen; Red-Oxygen; Cyan-Zr)

**Table S6.** HOMO – LUMO energies of the 2,4,6-TNP loaded **1**.

MOF with analyte	HOMO (eV)	LUMO (eV)	Energy gap (eV)
Zr-MOF	-1.52	-0.72	0.80
Zr-MOF + 1 TNP	-1.42	-0.75	0.67
Zr-MOF + 2 TNP	-1.20	-0.55	0.64
Zr-MOF + 3 TNP	-1.07	-0.02	1.05
Zr-MOF + 4 TNP	-0.99	-0.65	0.35

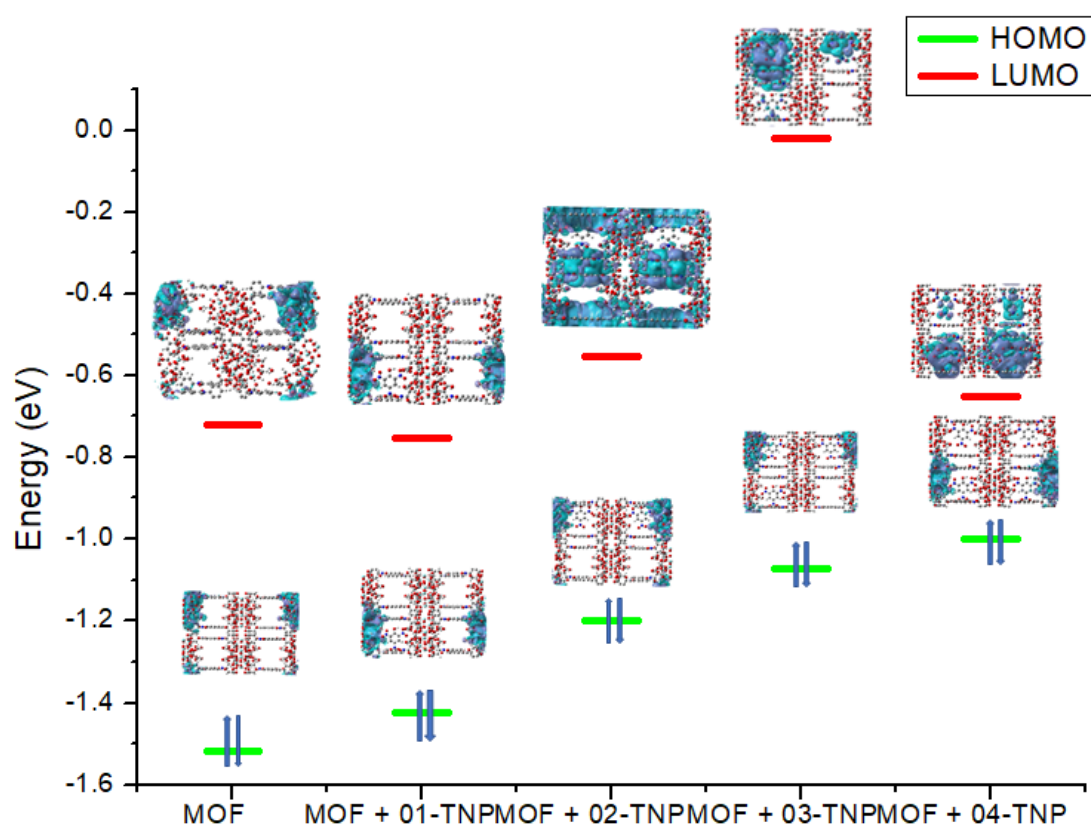


**Figure S26:** HOMO and LUMO energy plot for Zr-MOF and 2,4,6-TNP loaded **1**

**Table S7.** HOMO – LUMO energies of the 2,4,6-TNP loaded bare system.

Number of TNP molecule	HOMO (eV)	LUMO (eV)	Energy gap (eV)
<b>1</b>	-7.30	-4.91	2.39
<b>2</b>	-7.22	-4.79	2.43
<b>3</b>	-7.07	-4.71	2.36
<b>4</b>	-6.94	-4.62	2.32

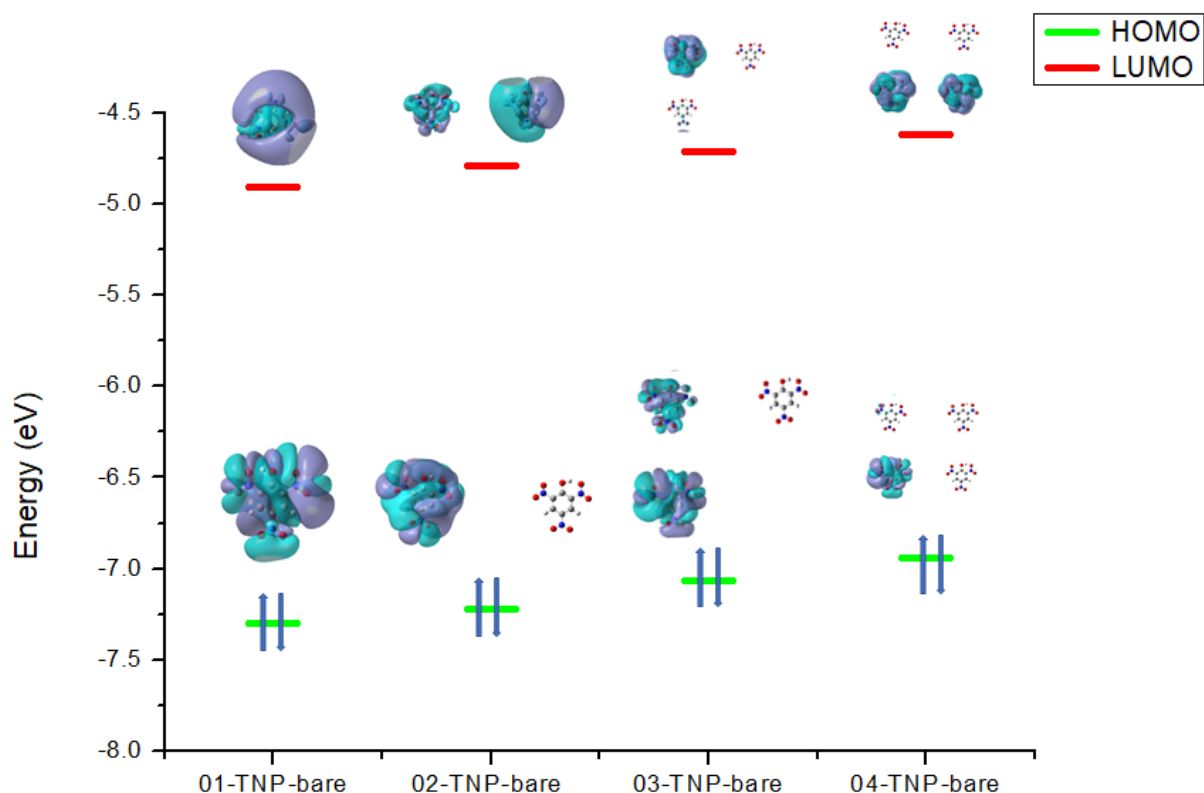


**Figure S27:** HOMO and LUMO energy plot for 2,4,6-TNP molecules.

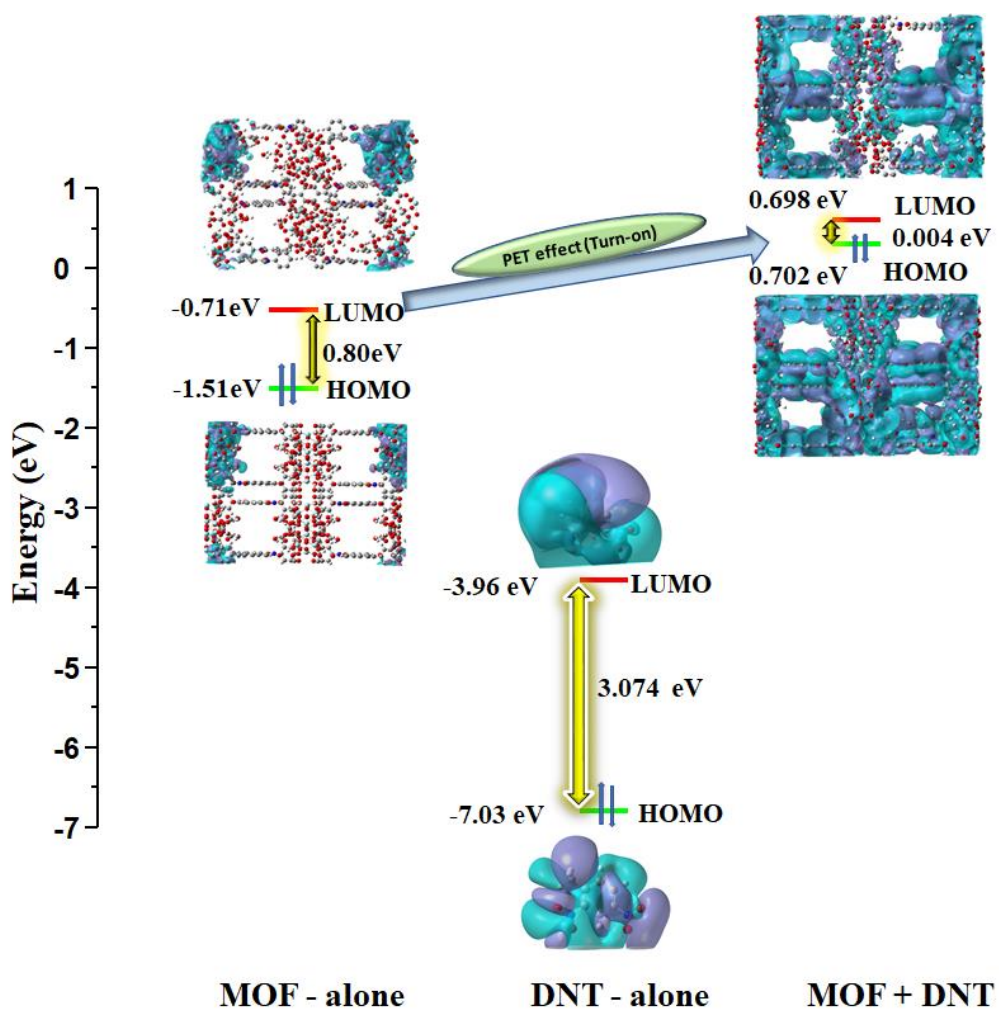


**Figure S28:** HOMO and LUMO energy plot for 1, DNT substrate and DNT loaded **1**.

**Table S8.** HOMO – LUMO energies of the 1, DNT and **1** with one DNT substrate.

Name of analyte and substrate	HOMO (eV)	LUMO (eV)	Energy gap (eV)
<b>1</b>	-1.52	-0.72	0.80
<b>DNT</b>	-7.038	-3.963	3.07
<b>1 + DNT</b>	0.7022	0.6985	-0.004

## References:

1. J. P. Perdew, *Phys. Rev. B*, 1986, **33**, 8822–8824.
2. J. P. Perdew, K. Burke and M. Ernzerhof, *Phys. Rev. Lett.* 1996, **77**, 3865–3868.
3. J. Vandevondele, M. Krack, F. Mohamed, M. Parrinello, T. Chassaing and J. Hutter, *Comput. Phys. Commun.* 2005, **167**, 103–128.
4. J. VandeVondele and J. Hutter, *J. Chem. Phys.* 2003, **118**, 4365–4369.
5. G. Lippert, J. Hutter and M. Parrinello, *Theor. Chem. Acc.* 1999, **103**, 124–140.
6. G. Lippert, M. Parrinello and J. Hutter, *Mol. Phys.* 1997, **92**, 477–487.
7. J. VandeVondele and J. Hutter, *J. Chem. Phys.* 2007, **127**, 114105.
8. S. Goedecker, M. Teter and J. Hutter, *Phys. Rev. B*, 1996, **54**, 1703–1710.
9. S. Grimme, J. Antony, S. Ehrlich and H. Krieg, *J. Chem. Phys.* 2010, **132**, 154104–154122.
10. S. S. Nagarkar, A. V. Desai and S. K. Ghosh, *Chem. Commun.* 2014, **50**, 8915–8918.
11. Y. Rachuri, B. Parmar, K.K. Bisht and E. Suresh, *Dalton Trans.* 2016, **45**, 7881–7892.
12. B. Wang, X.-L. Lv, D. Feng, L.-H. Xie, J. Zhang, M. Li, Y. Xie, J.-R. Li and H.-Cai. Zhou, *J. Am. Chem. Soc.* 2016, **138**, 6204–6216.
13. S. Mukherjee, A.V. Desai, B. Manna, A.I. Inamdar and S.K. Ghosh, *Cryst. Growth Des.* 2015, **15**, 4627–4634.
14. S. K. Mostakim and S. Biswas, *CrystEngComm.* 2016, **18**, 3104–3113.
15. S. S. Nagarkar, B. Joarder, K.C. Abhijeet, M. Soumya and S.K. Ghosh, *Angew. Chem. Int. Ed.* 2013, **52**, 2881–2885.
16. S.S. Nagarkar, A.V. Desai, P. Samantaa and S.K. Ghosh, *Dalton Trans.* 2015, **44**, 15175–15180.
17. J. Ye, L. Zhao, R.F. Bogale, Y. Gao, W. Xiaoxiao, X. Qian, S. Guo, J. Zhao and G. Ning, *Chem. Eur. J.* 2015, **21**, 2029 – 2037.
18. L. Hui Cao, F. Shi, W.-M. Zhang and S. Q. Zang, *Chem. Eur.J.* 2015, **21**, 15705 – 15712.
19. R. L. Joseph, Principles of Fluorescence Spectroscopy, 3<sup>rd</sup> ed, Springer. 2006.